Rigorous Hydrodynamic Description of Unmagnetized Multi-ion Plasmas

Andrei N. Simakov and Kim Molvig*

Los Alamos National Laboratory

***We acknowledge discussions with B. Albright and G. Kagan**

Kinetic Physics 2016 Workshop

Livermore, CA

April 5-7

LA-UR-16-21962

ICF Rad-Hydro Simulations Can Be Improved by Self-Consistently Including Plasma Transport Effects

- **Although plasma kinetic effects may be fundamentally important for certain ICF implosions, *some* missing plasma effects may be accounted for through fluid models**
- **Such effects include**
  - Differential motion and heating of various ion species
    - Capsule's fuel composition modifications
    - Mix at interfaces
    - Artificial stagnation features in hohlraums
  - Large physical plasma viscosity
    - Reduced capsule compression
    - Suppression of high-order modes
  - Multi-ion effects on electron heat transport
    - Reduced heat conductivity ~ $1/Z_{eff}$
  - …

Accounting for Ion Inter-Penetration Can Help Eliminate Artificial Stagnation Features in Hohlraums

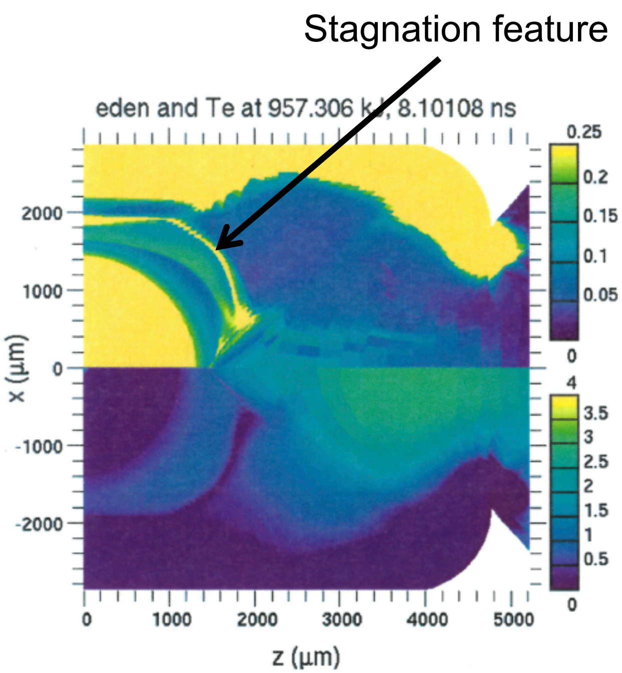

HYDRA predicts artificial stagnation features formed as ablated capsule and hohlraum plasmas interact

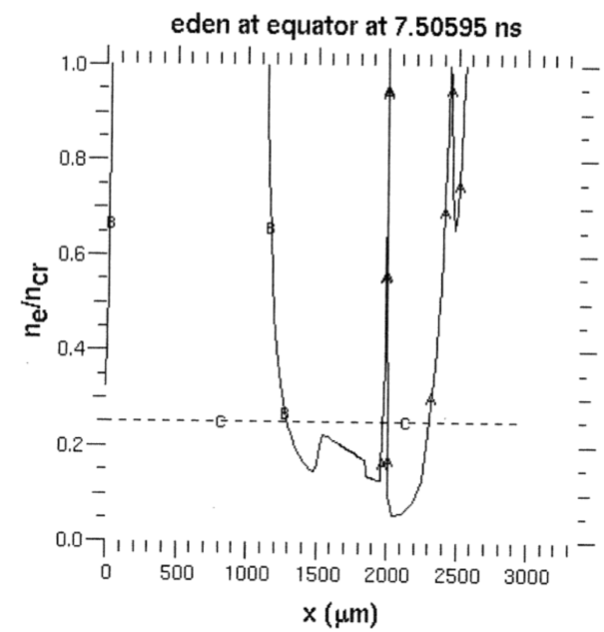

Inside the features, electron density exceeds $n_{critical}/4$, preventing laser from propagating further

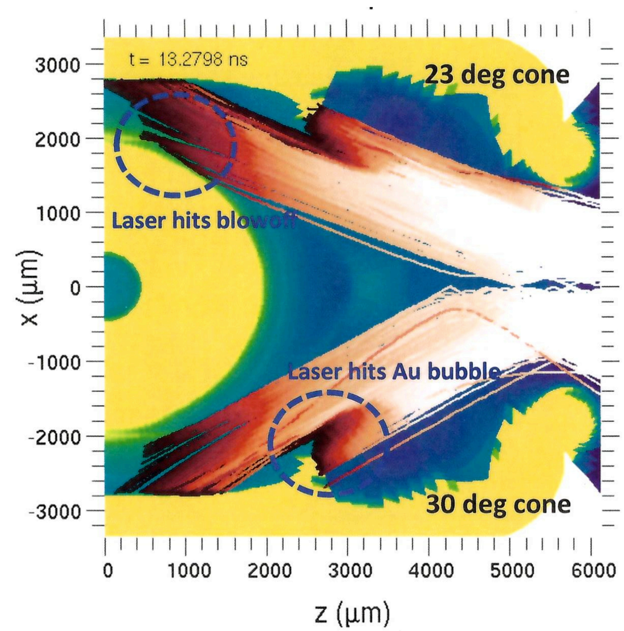

Laser energy deposition on the hohlraum wall is modeled incorrectly, resulting in poorly predicted implosion shape

Physical Ion Viscosity Can Reduce Fuel Compression, Suppress High-Order Modes

$$Re \sim \frac{V}{v_{thi}} \frac{1}{Kn} \sim \frac{V}{300[\mu m/ns]\sqrt{T_i[keV]}} \frac{1}{Kn}$$

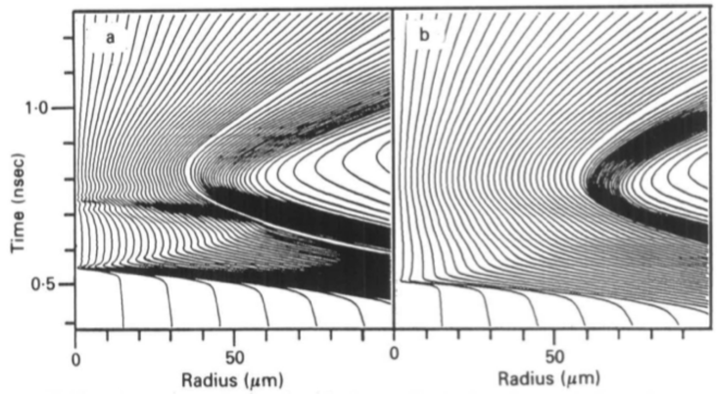

FIGURE 1. Fluid trajectories calculated with (a) artificial viscosity and (b) real viscosity with non-LTE model. In (a), the first shock wave arrives at 0·55 nsec and is reflected back to the pusher. In (b), however, this reflected shock and other subsequent shock waves do not show up.

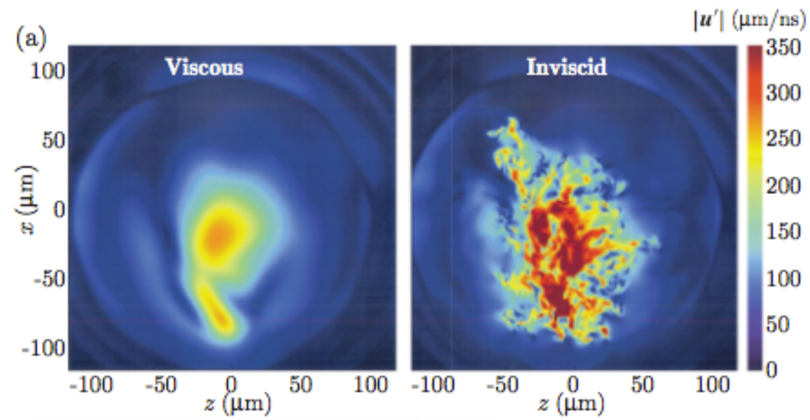

FIG. 4. (Color online) Viscous effects on the fluctuating velocity. (a) Fluctuating velocity magnitude at 22.21 ns with (left) and without (right) viscosity. (b) Kinetic energy spectra in the hot spot from the

Yabe *et al.*, Las. Part. Beams **7**, 259 (1989);

also Mason *et al.*, PoP **21**, 022705 (2014);

also Vold *et al.*, PoP **22**, 112708 (2015)

Weber *et al.*, PRE **89**, 053106 (2014);

also Haines *et al.*, PoP **21**, 092306 (2014)

Hydrodynamic Plasma Descriptions Have Long History

- **The best known for single ion plasmas is due to Braginskii (1957)**
  - Used the Chapman-Enskog approach
- **Zhdanov used Grad's 21-moment method for multiple ion plasmas (1980s)**
  - Extremely difficult to understand due to cumbersome notation
- **Albright and Daughton, Zimmerman obtained semi-phenomenological descriptions of unmagnetized multiple ion plasmas**
- **Amendt *et al.*, Kagan *et al.* studied diffusive ion fluxes in binary mixtures**
- **Simakov, Molvig, and Vold recently obtained a *rigorous* description of unmagnetized plasmas with arbitrary number of arbitrary ion species**
  - Employed the Chapman-Enskog approach and asymptotic expansion in Kn<<1
  - Electron and ion treatments decouple due to $m_e/m_i \ll 1$
  - Allow $T_e \neq T_i$; ions have same temps. $T_i = T$ but slightly different flows $u_i = u + V_i$, $|V_i| \ll u$
  - Results reduce to those of Braginskii for single ion species plasmas
  - Should be straightforward to implement in codes
  - Refs.: PoP **21**, 024503 and 092709 (2014); *ibid.* **23**, 032115 and 032116 (2016)

Plasma Evolution is Described by Conservation Equations to O(Kn²)

- **Total mass, momentum, and energy conservation equations are**

$$\frac{\partial \rho}{\partial t} + \boldsymbol{\nabla} \cdot (\rho \boldsymbol{u}) = 0,$$

$$\frac{\partial (\rho \boldsymbol{u})}{\partial t} + \boldsymbol{\nabla} \cdot \left(\rho \boldsymbol{u}\boldsymbol{u} + p \overleftrightarrow{I} + p_e \overleftrightarrow{I} + \overleftrightarrow{\pi} + \overleftrightarrow{\pi}_e \right) = 0,$$

$$\frac{\partial}{\partial t}\left[\frac{3}{2}(p + p_e) + \frac{1}{2}\rho u^2\right] + \boldsymbol{\nabla} \cdot \left[\frac{5}{2}\left(\sum_i p_i \boldsymbol{u}_i + p_e \boldsymbol{u}_e\right) + \frac{1}{2}\rho u^2 \boldsymbol{u} + \boldsymbol{q} + \boldsymbol{q}_e + \left(\overleftrightarrow{\pi} + \overleftrightarrow{\pi}_e\right) \cdot \boldsymbol{u}\right] = \boldsymbol{E} \cdot \boldsymbol{J} = 0.$$

- **To close need electron and ion heat fluxes, viscosities, drift velocities, and equation for electron pressure**
- **Keep electron viscosity in high-Z plasmas:** $|\vec{\pi}_C|/|\vec{\pi}_e| \sim Z_C^{-4}\sqrt{A_C m_p/m_e} \sim 0.1$
- **Here, concentrate on ions**

Ion Diffusion Velocities V_i, Heat Flux q, and Viscous Stress Tensor π Are Given to O(Kn) by

$$\begin{pmatrix} \boldsymbol{V}_1 \\ \boldsymbol{V}_2 \\ \cdots \\ \boldsymbol{V}_N \\ \boldsymbol{q}/p \end{pmatrix} = -\begin{pmatrix} \Delta_{11} & \Delta_{12} & \cdots & \Delta_{1N} & D_{T1} \\ \Delta_{21} & \Delta_{22} & \cdots & \Delta_{2N} & D_{T2} \\ \cdots & \cdots & \cdots & \cdots & \cdots \\ \Delta_{N1} & \Delta_{N2} & \cdots & \Delta_{NN} & D_{TN} \\ D_{T1} & D_{T2} & \cdots & D_{TN} & \kappa/n \end{pmatrix} \cdot \begin{pmatrix} \boldsymbol{d}_1 \\ \boldsymbol{d}_2 \\ \cdots \\ \boldsymbol{d}_N \\ \nabla \log T \end{pmatrix},$$

$$\sum_i \rho_i \boldsymbol{V}_i = 0,$$

$$\boldsymbol{d}_i = \boldsymbol{\nabla}\left(\frac{n_i}{n}\right) + \left(\frac{n_i}{n} - \frac{\rho_i}{\rho}\right)\boldsymbol{\nabla}\log p + \left(\frac{Z_i n_i}{n_e} - \frac{\rho_i}{\rho}\right)\frac{\boldsymbol{\nabla} p_e}{p} + \left(\frac{Z_i n_i}{n_e} - \frac{Z_i^2 n_i}{\sum_j Z_j^2 n_j}\right)\frac{\beta_0 \boldsymbol{\nabla} T_e}{T}$$

- Require generalized diffusion coeffs. Δ_{ij}', thermo-diffusion (Soret) coeffs. D_{Ti}, Dufour coeffs. D_{Ti}', and heat conduction coeff. *κ*
- Viscosity is $\overleftrightarrow{\pi} = -\eta \overleftrightarrow{W}, \ \overleftrightarrow{W} \equiv \boldsymbol{\nabla u} + (\boldsymbol{\nabla u})^T - \frac{2}{3}(\boldsymbol{\nabla} \cdot \boldsymbol{u}) \overleftrightarrow{I}$, require viscosity coeff. *η*

To Evaluate Ion Transport Coeffs. Require O(Kn) Correction f_i^1 to Ion Maxwellian Distribution Functions

- **The corrections are solutions of *Spitzer problems* $C_i(f_i^1)$=known, i=1,…,N with C_i linearized collision operator for species i with all ion species**
- **Can expand f_i^1 in polynomials, find expansion coeffs. variationally**
  - The variational functionals are maximized by the Spitzer solutions, with maximum values equal to entropy production sources
  - Plasma transport coeffs. are known functions of expansion coeffs. and possess quadratic accuracy compared with trial functions
  - Expansion coeffs.
    - are obtained by solving linear systems of 3N equations (for drift velocities and heat flux) or 2N equations (for viscosity)
    - depend on pair-wise ratios of ion masses $\mu_{ij} \equiv \frac{m_j}{m_i}$, charges $\zeta_{ij} \equiv \frac{Z_j^2 \log \Lambda_{ij}}{Z_i^2 \log \Lambda_{ii}}$, and number densities $\frac{n_j}{n_i}$
- **Can solve linear systems numerically for any N; solved analytically for**
  - Single ion plasma ➔recover Braginskii
  - Two ion plasmas: (i) D+T, (ii) ions with disparate masses
  - Three ion plasma: D+T+gold

Example: Heat Conduction and Viscosity Coeffs. for Deuterium + Tritium Plasma

- **Introduce dimensionless coefficients** $\kappa = \dfrac{n_1 v_{th1}^2}{\nu_{11}}\hat{\kappa}, \quad \eta = \dfrac{p_1}{\nu_{11}}\hat{\eta}$
- **By going from pure D to pure T plasma, heat conduction is suppressed by $\sqrt{3/2}$, while viscosity increases by $\sqrt{3/2}$**

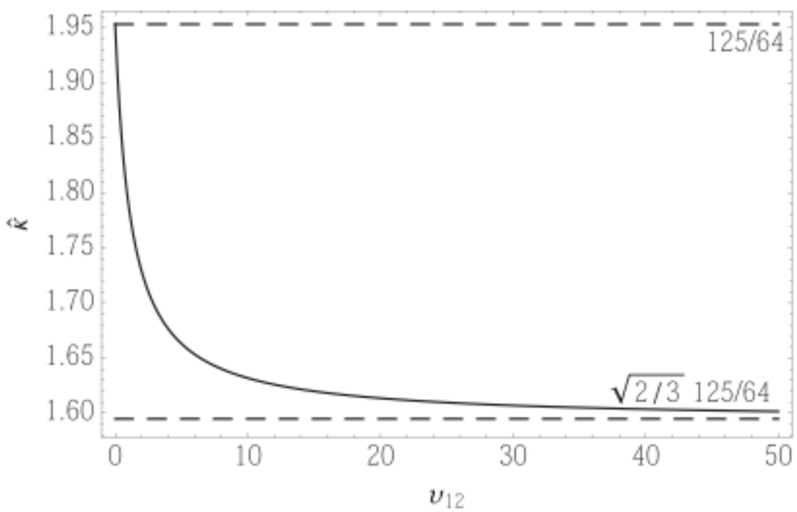

FIG. 2. The dimensionless heat conduction coefficient $\hat{\kappa}$ (solid) vs. the number density ratio $\upsilon_{12} = n_T/n_D$ for a deuterium-tritium plasma. The asymptotic values 125/64 (pure deuterium) and $(125/64)\sqrt{2/3}$ (pure tritium) are shown with dashed lines.

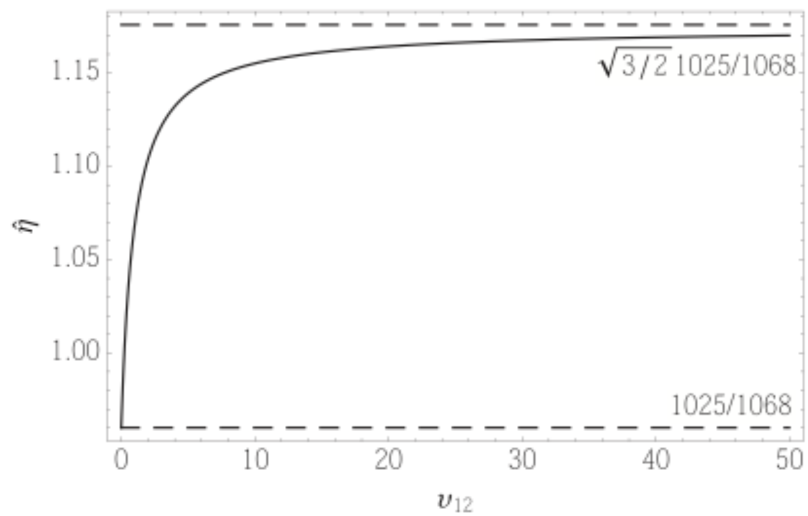

FIG. 3. The dimensionless viscosity coefficient $\hat{\eta}$ (solid) vs. the number density ratio $\upsilon_{12} = n_T/n_D$ for a deuterium-tritium plasma. The asymptotic values 1025/1068 (pure deuterium) and $(1025/1068)\sqrt{3/2}$ (pure tritium) are shown with dashed lines.

Example: Heat Conduction and Viscosity Coeffs. for Deuterium + Gold Plasma

- **By going from pure D to pure Au, ion heat conduction and viscosity get suppressed by** $\sqrt{\frac{m_D}{m_{Au}}}\left(\frac{Z_D}{Z_{Au}}\right)^4$ **and** $\sqrt{\frac{m_{Au}}{m_D}}\left(\frac{Z_D}{Z_{Au}}\right)^4$ **, respectively**

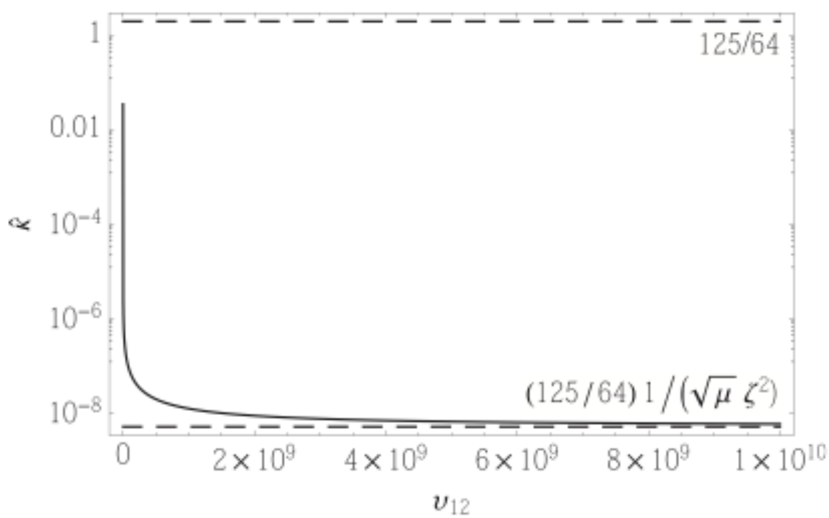

FIG. 5. The dimensionless heat conduction coefficient $\hat{\kappa}$ (solid) vs. $\upsilon_{12} = (n_{Au}/n_D)(Z_{Au}/Z_D)^2$ for a deuterium-gold plasma. The asymptotic values 125/64 (pure deuterium) and $(125/64)\sqrt{A_D/A_{Au}}(Z_D/Z_{Au})^4$ (pure gold) are shown with dashed lines.

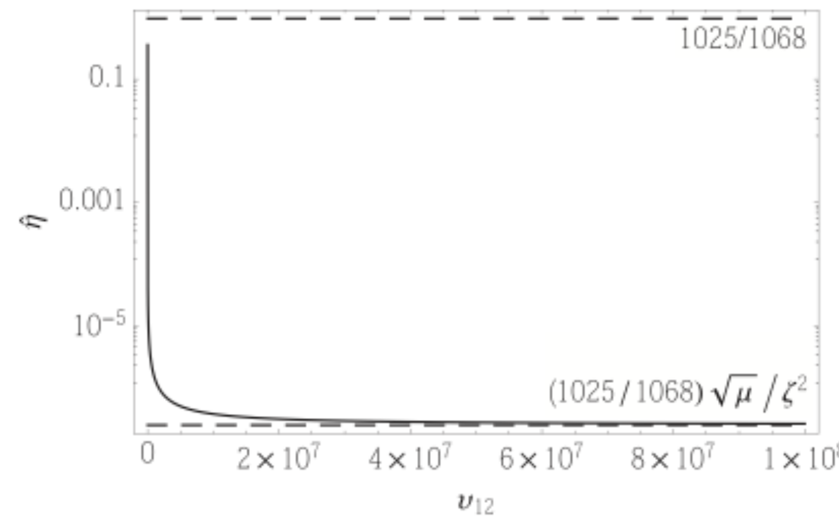

FIG. 6. The dimensionless viscosity coefficient $\hat{\eta}$ (solid) vs. $\upsilon_{12} = (n_{Au}/n_D)(Z_{Au}/Z_D)^2$ for a deuterium-gold plasma. The asymptotic values 1025/1068 (pure deuterium) and $(1025/1068)\sqrt{A_{Au}/A_D}(Z_D/Z_{Au})^4$ (pure gold) are shown with dashed lines.

Conclusions

- We obtained accurate hydrodynamic description of unmagnetized plasma with arbitrary number of arbitrary ion species by carrying out rigorous asymptotic expansion in Kn<<1
- Plasma transport coefficients depend on pair-wise ratios of ion masses, charges, and number densities and can generally be obtained by numerically solving small linear systems
- We obtained analytical expressions for the transport coefficients for several important cases
- The method recovers the Braginskii results for single ion plasma
- The hydrodynamic description accounts for several important plasma effects typically neglected in standard ICF simulations